Journal of Robotics and Control (JRC)
Volume 6, Issue 3, 2025
ISSN: 2715-5072 DOI: 10.18196/jrc.v6i3.26361

Effect of Liquid Height on Sloshing Dynamics in Cylindrical Containers Using H-Infinity Control with Smooth Velocity Input

Udomsak Jantontapo [1], Panya Minyong [2*], Songtham Deewanichsakul [3], Phichitphon Chotikunnan [4*], Rawiphon Chotikunnan [5], Nuntachai Thongpance [6]
[1, 2, 3] Mechatronics and Robotics Engineering established under the Faculty of Technical Education, Rajamangala University of Technology Thanyaburi, Pathum Thani, Thailand
[4, 5, 6] College of Biomedical Engineering, Rangsit University, Pathum Thani, Thailand
Email: [1] udomsak_j@rmutt.ac.th, [2] panya_m@rmutt.ac.th, [3] songtham_d@rmutt.ac.th, [4] phichitphon.c@rsu.ac.th, [5] rawiphon.c@rsu.ac.th, [6] nuntachai.t@rsu.ac.th
*Corresponding Author

***Abstract*—The research analyzes the dynamics of liquid sloshing in cylindrical containers, emphasizing the influence of liquid height on system stability and motion via H-Infinity Control methodologies. The main goal is to analyze how changes in liquid height affect the dynamics and stability of fluid transport systems and to assess the effectiveness of H-Infinity control in reducing sloshing effects. A simulation investigation was performed at different liquid levels using trapezoidal velocity profiles, including step inputs and gradual transitions. Performance was assessed using the Integral of Absolute Error (IAE) and Root Mean Square Error (RMSE). The results demonstrate that heightened liquid levels significantly improve sloshing dynamics, extend the settling time, and exacerbate inaccuracies in measurements due to increased fluid inertia. Smooth velocity profiles reduce sudden changes; yet, they cannot completely eliminate the destabilizing effects caused by large amounts of liquid. The study confirms a mechanical model for sloshing dynamics integrated with robust H-infinity control, providing significant insights for improving fluid management in robotics and automated systems. Subsequent research should encompass varied container designs, fluid characteristics, and sophisticated adaptive control methodologies.**

Keywords—Liquid Height Effects; Cylindrical Container Sloshing; H-Infinity Control; Smooth Velocity Profiles; Fluid Transport Stability.

I. INTRODUCTION

Creating and managing robotic and automation systems, such as medical manipulators, industrial robotic arms, and mobile robots, requires careful attention to how they move, how fast they respond, and how well they follow their paths in changing and uncertain situations. A significant issue occurs when these systems must transport liquids in partially filled containers, as agitation and motion can substantially impact their stability. When these systems have to move fluids in containers that are only partially filled, there is a serious issue because agitation and motion can substantially impact their stability. In these conditions, achieving precise motion control becomes increasingly difficult due to the unpredictable behavior of the fluid mass. Although several prior research works do not explicitly investigate fluid sloshing phenomena, they underscore the importance of establishing robust and adaptive control systems in environments vulnerable to shocks. This work includes using the best Proportional-Integral-Derivative (PID) controllers [1], smart algorithm-based methods to optimize systems [2], combining data from different sensors to estimate motion [3], and using advanced feedback and sliding mode controllers for stabilizing motors [4], [5]. These methodologies together offer critical insights into how control strategies improve system stability and responsiveness in real-time robotic applications. Multiple research projects have examined the ability of intelligent control systems to regulate the dynamic and complex behaviors shown by robots and mechatronic devices. Fuzzy-PID and neuro-fuzzy controllers have been very effective at reducing shaking and making systems like brushless DC (BLDC) motors, lane-keeping control systems, and robotic arms more stable, especially when they face complicated and unexpected situations. Fuzzy-PID and neuro-fuzzy controllers have demonstrated remarkable efficacy in reducing oscillations and enhancing stability in systems such as Brushless DC (BLDC) motors, lane-keeping control systems, and robotic arms, particularly in the presence of complex and unpredictable inputs [6]–[10]. Furthermore, Particle Swarm Optimization (PSO) and other advanced algorithms have been included in control systems to autonomously adjust PID parameters, hence improving their flexibility and responsiveness across many circumstances [11]–[13]. However, even with these improvements, traditional and smart management methods still struggle with fluid sloshing issues, especially when the shape of the container changes or when the fluid behaves in complex ways. This study aims to tackle these issues by looking at how the shape of the container and changes in liquid height affect sloshing in partially filled cylindrical containers; it also explains the benefits of using an H-infinity control framework to reduce sloshing effects.

Researchers have developed various advanced control algorithms to address the complexities of uncertain and nonlinear systems. This collection features traditional PID tuning methods and more advanced control techniques, like fuzzy logic, neuro-fuzzy inference systems, and rule-based expert systems [14]–[27]. Genetic Algorithms (GA) and especially Particle Swarm Optimization (PSO) are commonly used to improve PID settings, resulting in better adaptability, faster response times, and more stability in different working conditions [14]–[17]. Simultaneously, fuzzy expert systems

have demonstrated significant effectiveness in several decision-making applications. For instance, they have been employed in the classification of power system disturbances [18] and in medical diagnostics, including the diagnosis of carpal tunnel syndrome [19], heart failure [20], chemotherapy scheduling [21], and chronic kidney disease [27]. These systems frequently rely on fuzzy inference techniques or incorporate artificial neural networks to form neuro-fuzzy inference systems (NFIS), which excel in handling uncertain, imprecise, and nonlinear situations [24]–[26]. Fuzzy expert systems, when integrated with adaptive learning frameworks, evolve into sophisticated control structures capable of managing extremely dynamic systems. Consequently, they create a solid foundation for the advancement of clever and resilient controllers. These controllers are particularly important in fluid transport systems, where outside factors and changing interactions between the fluid and structure greatly affect how well they work and how stable they are.

Recent advances in smart control have combined methods like genetic algorithms, fuzzy logic controllers, and Adaptive Neuro-Fuzzy Inference Systems (ANFIS) to enhance performance in complicated and changing situations. Several fields, such as solar energy systems, robotic manipulators, intelligent navigation, and healthcare robotics, have applied these methodologies [28]–[43]. In these applications, control systems must demonstrate noise resistance, flexibility to nonlinear dynamics, and high-precision tracking capabilities. Neuro-fuzzy control techniques have been effectively applied in wrist rehabilitation robots [41], underwater robotic manipulators [37], and adaptive robotic arms with numerous degrees of freedom [38], [40]. Likewise, advancements in fuzzy-PID controllers have improved servo motor responsiveness [34], force-position hybrid control [35], and performance stabilization in hybrid power systems [39]. These advances have markedly advanced the development of adaptive and learning-based control systems in practical applications. Moreover, Iterative Learning Control (ILC) has proven to be an efficient technique for overseeing repeated robotic operations, including path tracking, soft tissue contact, and nonlinear trajectory acquisition, especially within the domain of medical robotics [44]–[46]. Complementary research has yielded hardware-efficient fuzzy-PI/PID controllers and adaptive fuzzy systems designed for real-time functionality, hence improving energy economy and control responsiveness in actuator-based platforms [47]–[50]. The applicability of fuzzy logic encompasses several technical fields. It has been utilized in maximum power point tracking (MPPT) algorithms for solar systems [51], optimization of indoor air quality in critical situations [52], and spacecraft orbital modifications under input limitations and gain variations [53]. These studies highlight how useful and effective fuzzy logic is for solving complex control problems that are affected by real-life conditions. A plethora of research initiatives have examined robotic systems functioning in restricted areas concerning motion control and trajectory planning. This initiative encompasses the creation of robotic arms for COVID-19 specimen collecting [54], manipulators employing inverse kinematics techniques [55], and multi-axis robots programmed by GRBL platforms [56]. Despite these developments, limited study has examined the interaction between smart control systems and fluid sloshing, especially concerning various container geometries. The behavior of the fluid in these systems is significantly affected by the form of the container and the depth of the liquid, which determine the frequency and amplitude of the resultant sloshing motion. These discrepancies can significantly affect the system's inertial response, influencing control design. This situation highlights the need for establishing strong control systems that can adjust to changes in fluid dynamics, container sizes, and external factors, which are essential for improving the stability and precision of fluid movement in robotic applications.

Recent studies on motion planning and calibration in unpredictable settings, like crowded areas and differential-drive robotic systems, have provided useful information on managing movement uncertainty [57]. However, robotic fluid transport systems have not directly applied this research to reduce sloshing. Nevertheless, robotic fluid transport systems have not directly applied this study for sloshing minimization. Likewise, fundamental research in mechatronic system control using multi-fingered robotic hands and linear motor platforms provides theoretical insights pertinent to modeling system inertia and trajectory dynamics in sloshing-prone situations [58]. The field of intelligent control has progressed significantly in recent times, especially in trajectory tracking, adaptive PID tuning, fuzzy logic control, and Adaptive Neuro-Fuzzy Inference Systems (ANFIS) for robotic manipulation [59], [60]. Innovative techniques have produced genetic algorithm-optimized LQR controllers for balancing applications [61] and fuzzy LQR-PID controllers for stabilizing bipedal robots across diverse height configurations [62]. Many of these designs, however, assume fixed or rigid container structures, which limits their effectiveness in managing the fluid dynamics associated with sloshing behavior. Alternative control frameworks, like dual PID controllers [63], adaptive parallel iterative learning control schemes [64], and fuzzy controllers with configurable membership functions [65], demonstrate considerable versatility in tackling nonlinear control issues. However, we have not applied these strategies to fluid-structure interaction problems. Expert systems enhanced with gain-scheduling approaches and fault-tolerant multi-agent architectures exhibit robustness in complex scenarios [66]; yet, they do not directly address sloshing dynamics. Many researchers have utilized Takagi–Sugeno fuzzy models to depict systems with variable damping and stiffness [67], whereas ANFIS architectures have been applied in autonomous navigation systems, humanoid robotics, and robotic manipulators [68], [69]. These findings have collectively broadened the theoretical foundations of adaptive control. T The integration of H-infinity (H∞) control with sloshing dynamics remains poorly investigated in contemporary research. Despite the effectiveness of various robust control methodologies, such as fuzzy logic, PID, and neurofuzzy approaches, in alleviating disturbances and managing nonlinearities [70]–[73], they often face difficulties in situations marked by highly nonlinear fluid dynamics or considerable model uncertainties. On the other hand, H-infinity control provides a solid mathematical method to reduce the worst effects of disturbances, which makes it especially useful for handling fluid sloshing in different container shapes and liquid heights. This study fills a significant research gap by proposing an H-infinity-based method to mitigate fluid oscillation under dynamic conditions. Extensive research on intelligent control in robotics and mechatronics has markedly progressed the development of control theory [74]. Innovations like fuzzy root locus optimization [75] and type-2 fuzzy hierarchical control methodologies [76] have proven effective for nonlinear systems. Open-closed-loop Iterative Learning Control (ILC)

frameworks have been used in medical robotics [77], while fuzzy-based ILC setups have been devised for intricate manipulator systems [78]. Recent developments encompass fuzzy-neuro hybrid controllers in hybrid force-position systems [79] and dynamic trajectory planners for mobile robot navigation in highly constrained environments [80]. Moreover, adaptive PID controllers have been effectively utilized in essential systems like nuclear reactors, DC converters, and smart microgrids [81]–[84]. Besides motion control, fuzzy reasoning techniques have been employed in electric vehicle charging systems [85], decision-making algorithms, and swarm-based control inside mobile robot networks [86]. Even though there are many uses for it, not much research has looked into how to combine intelligent control systems with fluid sloshing dynamics, particularly when dealing with different container shapes and liquid levels. This work underscores the necessity for a robust control technique capable of addressing the nonlinearities and uncertainties inherent in fluid sloshing. Even though current control methods like fuzzy, PID, and neuro-fuzzy models can help reduce problems, they may not consistently guarantee optimal performance in the worst situations. In contrast, H-infinity (H∞) control provides a mathematically valid framework for alleviating the impacts of external disturbances and model uncertainty. Thus, it is effective at reducing fluid sloshing in dynamic environments. The main research need is that H∞ control frameworks are not often used in fluid transport systems affected by changing interactions between fluids and structures. This work aims to study how changes in liquid height and movement patterns affect sloshing while also introducing an H∞-based control method to effectively reduce swaying and improve system stability.

The research contributes to how fluids move up and down in cylindrical containers with different fluid levels and speeds, using a strong control method called H-infinity. This approach was chosen for its robust ability to mitigate disturbances and control model inaccuracies, crucial for handling dynamic fluid-structure interactions. Three sorts of motion profiles are evaluated: a step input, a moderate ramp with a five-second climb, and a rapid ramp with a two-and-a-half-second rise. The fluid levels fluctuate between 0.05 m and 0.20 m. The effectiveness of the control system in mitigating fluctuations is evaluated using the Integral of Absolute Error (IAE) and Root Mean Square Error (RMSE). The study provides important information for creating transport systems that are more stable and flexible by looking at how inertia, damping effects, sloshing amplitude, input velocity, and fluid height are connected. These discoveries provide a solid foundation for enhancing fluid management in robotics, healthcare, and autonomous systems operating in dynamic and unpredictable environments.

II. Research Method

The aim of this project is to develop and implement a complete framework for mitigating whirling effects in fluid transport systems using H-infinity control techniques. The suggested technique guarantees dynamic stability through real-time feedback and strong control mechanisms, effectively tackling the issues of fluctuating liquid levels and diverse container sizes.

Fig. 1 illustrates the sequential phases of the research approach. The initial phase of the process involves identifying the issue and establishing research objectives. A mathematical model for whirling dynamics is built utilizing pendulum approximations and wave equations. This methodology generates transfer functions and equations for natural frequency, crucial for comprehending fluid dynamics in cylindrical vessels.

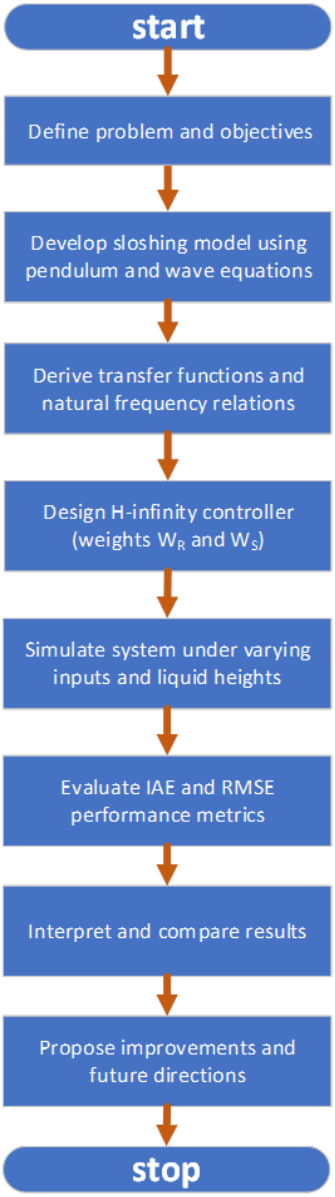

Fig. 1. Flowchart of the research process

Thus, the H-infinity controller is developed, utilizing uncertainty and sensitivity weights (W_R and W_S) to manage disturbances and guarantee reference tracking. The controller is utilized to simulate the system's behavior under various scenarios, including abrupt input alterations and gradual speed modifications as the liquid height fluctuates from 0.05 m to 0.20 m.

The system's performance is measured by looking at the Integral of Absolute Error (IAE) and Root Mean Square Error (RMSE) to check how well it tracks and how effectively it dampens. Researchers examine and compare the results with theoretical predictions and other studies. The results eventually support improvements and outline potential research directions to strengthen system resilience and practical utility.

III. TRANSPORTATION ROBOT

The advancement of mobile robots has garnered considerable interest in recent years, with applications spanning industries including transportation, exploration of challenging terrains, and operations in hazardous situations. The COVID-19 epidemic has expedited the utilization of service robots, especially for functions such as food delivery in restaurants and analogous service-related applications. Nevertheless, regulating the locomotion of robots in dynamic settings, such as traversing congested restaurant areas or hospital corridors, continues to pose a considerable problem.

This research centers on the development of a multifunctional service robot that can autonomously move products, including food and beverages in restaurants and necessary supplies in medical settings. In restaurant applications, the robot guarantees efficient and spill-free delivery of food and beverages, upholding hygiene and operational efficacy in dynamic and congested environments. In hospitals, the robot delivers meals, medications, and critical fluids to patients, alleviating the burden on medical personnel and minimizing human interaction to mitigate contamination risks. The robot's capacity to traverse securely and manipulate fragile objects in dynamic environments underscores its versatility and appropriateness for the service and healthcare sectors, consequently improving operational efficiency and overall service quality.

A. *Design and Structure of Mobile Robots*

The structural design of mobile robots is essential since it establishes the basis for the robot's operational capabilities and efficiency across many situations, as depicted in Fig. 2.

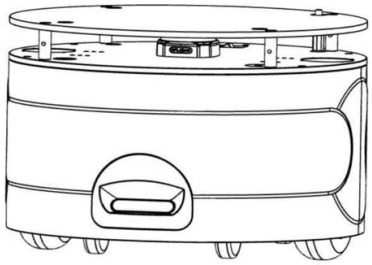

Fig. 2. Prototype of a transportation robot

To attain the necessary control depicted in Fig. 2, the integration of sophisticated control devices, as outlined in Fig. 3, is essential. The robot operates using a DC brushless motor, with position and speed regulation overseen by a microcontroller that gets directives from a mini-PC. The sensory apparatus includes a 3D camera for detecting its surroundings while moving and LiDAR technology for measuring distances and making a map of its surroundings using laser light.

The robot's structural design ensures efficient, safe, and sturdy operation across many settings. Dimensions, composition, stability, and safety are assessed to improve operational efficiency and longevity. The robot's size is tailored for navigation in restricted spaces, such as restaurant hallways, kitchens, or hospital corridors, possessing the agility to go around obstacles. The robot's construction components inhibit contamination by utilizing stainless steel for corrosion resistance and food-grade plastic to guarantee safety in culinary and medical settings.

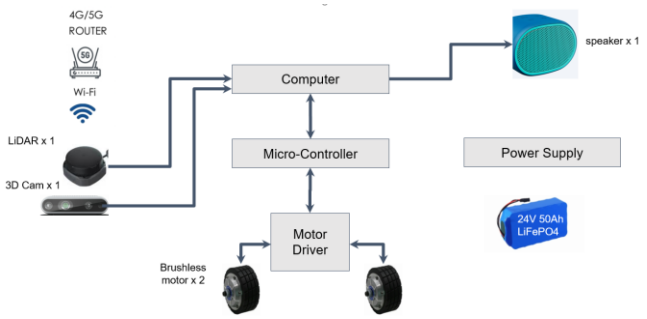

Fig. 3. Motion control circuit of the robot

The robot's design in medical applications caters to tasks like transporting meals, medications, and medical supplies within hospitals. A low center of gravity improves stability during transportation, especially when transporting fragile things such as liquid pharmaceuticals or medical tools. The robot strategically positions components and batteries to maintain equilibrium and prevent tipping, a crucial aspect for the operations of both restaurants and hospitals. The robot's design also gets rid of sharp edges and dangerous parts in favor of rounded shapes to avoid collisions and lower the risk of harm in crowded places like hospital wards or patient rooms.

Fig. 4 illustrates how vibration isolation principles, using coil springs and shock absorbers as vibration-dampening mechanisms, achieve smooth motion. The robot features two drive motors and two supporting wheels for improved agility, as shown in Fig. 4, which presents the simulated assembly of the robot's components from both front and rear perspectives. This design allows the robot to function effortlessly in both service and medical settings, guaranteeing efficiency, safety, and dependability.

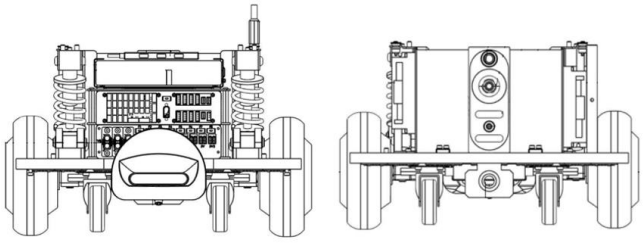

Fig. 4. Simulated assembly of robot components

B. *Robot Motion and Dynamics*

This study investigates a mobile robot with two independently powered wheels that use a differential drive to rotate without slipping or lateral displacement. The robot is additionally outfitted with two auxiliary wheels at both the front and rear. The motion plane's reference frame is depicted in Fig. 5.

Fig. 5 illustrates the robot's movement, with the reference frame's position specified by (x, y, θ).

The robot's linear and angular velocities can be determined using the following references [84], [85], and linear velocity v can be calculated from the angular velocities of the left and right wheels, as seen in (1).

$$v = r_{\omega} \frac{\omega_{\omega}^{l} + \omega_{\omega}^{r}}{2} \quad (1)$$

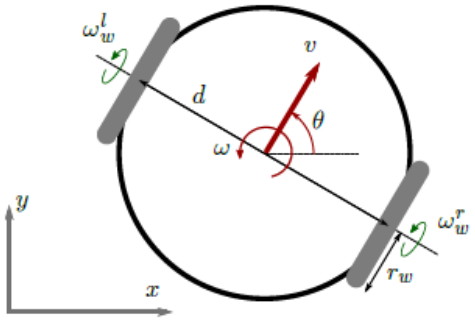

Fig. 5. Simulated assembly of robot components

In (2) illustrates that the difference in angular velocities (ω) of the left and right wheels determines the robot's angular velocity.

$$\omega = r_\omega \frac{\omega_\omega^r - \omega_\omega^l}{d} \tag{2}$$

where, r_ω is the radius of the left and right wheels, ω_ω^r is the angular velocity of the right wheel, ω_ω^l is the angular velocity of the left wheel, $d$is the distante between the left and right wheels.

The robot's position and orientation in relation to the base frame are contingent upon the type of motor controller employed. This study calculates the positional change along the x-axis and y-axis using (3) and (4), respectively.

$$\frac{dx}{dt} = v\,cos(\theta) \tag{3}$$

$$\frac{dy}{dt} = v\,sin(\theta) \tag{4}$$

The alteration in the robot's orientation can be determined using (5).

$$\frac{d\theta}{dt} = \omega \tag{5}$$

Here, θ denotes the angle between the robot and the x-axis of the reference frame. Consequently, the motion model of the system can be articulated in a simpler manner as (6).

$$\begin{bmatrix}\dot{x}\\ \dot{y}\\ \dot{\theta}\end{bmatrix} = \begin{bmatrix}cos(\theta) & 0\\ sin(\theta) & 0\\ 0 & 1\end{bmatrix}\begin{bmatrix}v\\ \omega\end{bmatrix} \tag{6}$$

C. Oscillation Reduction Control Theory

The motion of an object along a linear path is influenced by the interaction of time, velocity, and acceleration. In open containers, an increase in liquid velocity produces positive acceleration, while a reduction in velocity results in negative acceleration. This phenomenon relates to liquids in open containers; sloshing or surface oscillations occur, potentially causing the liquid to spill from the container. The extent of sloshing depends on the magnitude of the acceleration, irrespective of whether it is positive or negative. Making a controller that can filter out the acceleration frequencies that cause the water surface to oscillate could make it easier for liquids in open containers to move around, reducing spills and chaos.

It is necessary to use mathematical modeling to create controllers and a framework for analyzing how the oscillations of liquid in a mobile container change over time. The container's lateral acceleration allows us to model the liquid's motion as a pendulum system. Examining these equations enables the assessment of the responses of a liquid's surface and a pendulum to forces applied from multiple directions. This is essential for understanding the stability and regulation of complex systems in practical applications.

This study employs a cylindrical glass as the container for the liquid, as depicted in Fig. 6. and Fig. 7 provides a more detailed depiction of the container model from Fig. 6. The container accelerates horizontally (a), causing the liquid within to display surface oscillations. This behavior can be characterized by a pendulum system comprising mass (m) and length (l) within the container, as seen in Fig. 7. So, the sloshing motion of the liquid inside the cylinder-shaped container can be modeled by using the container's radius (R), the height (h_s), and acceleration (a) in the direction of the robot's movement.

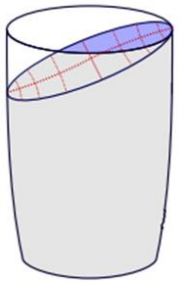

Fig. 6. The structure of the liquid container

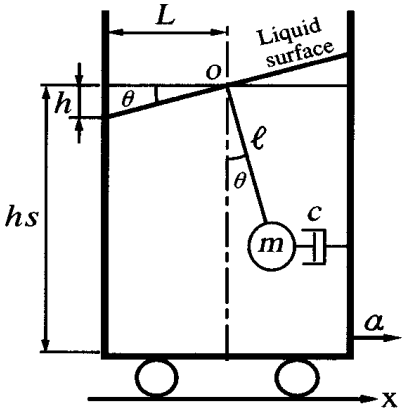

Fig. 7. Pendulum model of liquid surface oscillation

The sloshing dynamics of liquid in a cylindrical container can be examined under the assumptions of incompressibility, inviscidity, and irrotationality. Under these circumstances, the velocity potential ($\phi(r,\theta,z,t)$) adheres to the Laplace equation in cylindrical dimensions, as seen in (7).

$$\nabla^2\phi = \frac{1}{r}\frac{\partial}{\partial r}\left(r\frac{\partial\phi}{\partial r}\right) + \frac{1}{r^2}\frac{\partial^2\phi}{\partial\theta^2} + \frac{\partial^2\phi}{\partial z^2} = 0 \tag{7}$$

where, r is the represents the radial distance from the center of the cylinder. θ is the represents the angular coordinate. z is the represents the vertical coordinate.

From (7), for the scenario of the container wall ($r = R$), the velocity normal to the wall must be null, resulting in (8).

$$\frac{\partial\phi}{\partial r} = 0 \tag{8}$$

At the free surface ($z = h(t)$), the boundary conditions for kinematic and dynamic restrictions are specified by (9) and (10).

$$\frac{\partial \eta}{\partial t} = \frac{\partial \theta}{\partial z} \tag{9}$$

$$\frac{\partial \phi}{\partial t} + g\eta = -a\, sin(\phi) \tag{10}$$

where, $\eta(r, \theta, t)$ is the denotes the displacement of the free surface. a is the represents the horizontal acceleration of the container.

The oscillation of the liquid surface in the container can be modeled as a two-dimensional event, assuming gradual changes in acceleration. Fig. 7 illustrates how a pendulum model can depict this approximation. The governing equation is written as (11).

$$J\frac{d^2\theta}{dt^2} = -c\frac{d(l\theta)}{dt} l\, cos^2\theta - mgl\, sin\,\theta + mal\, cos\,\theta \tag{11}$$

This takes into account the moment equilibrium around the pendulum's pivot point.

where, J is the denotes the moment of inertia. θ is the denotes the angle formed between the horizontal line and the liquid surface. α is the represents the acceleration exerted on the container holding the liquid.

Upon linearizing (12), the motion equation is derived.

$$\ddot{\theta} = -\frac{c}{m}\dot{\theta} - \frac{g}{l}\theta + \frac{1}{l}\alpha \tag{12}$$

The sloshing model indicates that the natural frequency (h_s) of the system is associated with the liquid height and can be computed using (13) and whereas (k) may be determined using (14) for n equal to 1,2, ...

$$f_n = \frac{\sqrt{gk\, tanh(kh_s)}}{2\pi} \tag{13}$$

$$k = \frac{(\pi n)}{l_s} \tag{14}$$

This research centers on the construction of a robot motion control system that primarily addresses the sloshing of liquid within cylindrical containers. Fig. 7 illustrates the transfer function for the liquid sloshing dynamics, expressed as (15).

$$G(s) = \frac{\theta(s)}{F(s)} = \frac{R}{Js^2 + Bs + K} \tag{15}$$

where, $\theta(s)$ is the denotes the angle of liquid oscillation within the container. $F(s)$ is the force applied by the robot. R is the denotes the distance from the pivot point to the center of mass of the liquid. J is the moment of inertia. B is the damping coefficient. K is the stiffness coefficient.

The transfer function for the sloshing system is represented by (16) when the system is approximated as a second-order lag equation.

$$G(s) = \frac{K_s}{s^2 + 2\varsigma\omega_n s + \omega_n^2} \tag{16}$$

where, K_s is the system gain. ς is the damping ratio. ω_n is the natural frequency of the system.

This research utilizes a mechanical approach to simplify the complex wave-based model, improving its efficiency for use in embedded systems.

This function computes the natural frequency denoted by (17).

$$\omega_n = \sqrt{\frac{g \cdot k \cdot h_s}{L}} \tag{17}$$

where, g is the acceleration due to gravity (9.81 m/s^2). k is the swing constant (k≈1.841 for cylindrical containers). h_s is the liquid height. L is the represents the radius of the container.

This equation illustrates the relationship between oscillation, liquid height, and gravitational force, under the assumption that the system functions like a pendulum at small angles. It facilitates manageable modeling for real-time feedback regulation.

This equation, while not directly taken from the detailed wave dispersion relation (13), captures the main trend and was confirmed through performance analysis using simulations in this study.

The design of the control system for robotic mobility emphasizes reducing sloshing effects to facilitate effective liquid transport. The above equations and parameters are necessary to understand and control the system's dynamics, make sure stability, and improve the robot's ability to work reliably in changing environments.

IV. Feedback Control System Design with H_∞

A mobile robot attaches a container to the feedback control system to stabilize and reduce liquid sloshing. Fig. 8 demonstrates the utilization of the H-infinity controller to mitigate the impact of sloshing during the robot's movement. The H_∞ controller [86] is formulated to meet the mixed sensitivity criterion, as demonstrated in (18).

$$\left\| \begin{matrix} W_s S/\gamma \\ W_R R \end{matrix} \right\|_\infty < 1 \tag{18}$$

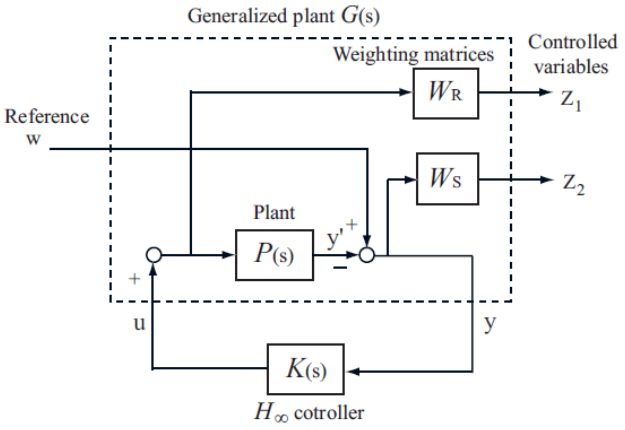

Fig. 8. Feedback control system with H_∞ controller

Fig. 8 shows that the feedback loop uses the H-infinity controller to control sloshing by reducing the impact of uncertainty in W_R and improving reference tracking through

the sensitivity function W_s. The architecture enables prompt adaptation to disturbances resulting from variable fluid inertia. In mobile robot navigation, this control approach is essential for managing unexpected acceleration patterns.

Weights for uncertainty (W_R) and sensitivity (W_s) are assigned due to the mixed sensitivity issue, which accounts for changes in model uncertainty. Model uncertainty is characterized as a perturbation term, as delineated in (19).

$$\Delta_p(s) = \tilde{P}(s) - P(s) \tag{19}$$

$\tilde{P}(s)$ represents the actual model, defined as $\tilde{P}(s) = P(s) + \Delta_P(s)$, where $P(s)$ is the nominal model. The closed-loop transfer function for robust stability is expressed as (20).

$$R(s) = K(s)(I - P(s)K(s))^{-1} \tag{20}$$

$K(s)$ denotes the controller. The small-gain theorem states that the closed-loop system maintains stability for all values of Δ_p, by if $\|\Delta_p R\|_\infty < 1$, which indicates that $\|W_R R\|_\infty < 1$. The frequency response of the transfer function $R(s) = K(s)(I - P(s)K(s))^{-1}$, which takes into account model uncertainty, is made better so that it can handle changes in the amount of liquid in the container and noise is cut down. To do this, the uncertainty weight (W_R) is incrementally elevated, as defined in (21).

$$W_R = \frac{10(5s+1)(10s+1)}{(s+40)(s+70)} \tag{21}$$

Likewise, the sensitivity weight (W_s) formulated for servo control to guarantee the robot precisely follows the reference position. In (22) presents the sensitivity weight transfer function (W_s).

$$W_s = \frac{950}{s + 10^{-4}} \tag{22}$$

The equations for the control system depicted in Fig. 8 are represented as (23) and (24).

$$\begin{bmatrix} z_1 \\ z_2 \\ y \end{bmatrix} = G(s) \begin{bmatrix} w_1 \\ u \end{bmatrix} \tag{23}$$

$$G(s) = \begin{bmatrix} 0 & W_R \\ W_S & P_{nom}W_s \\ -I & -P_{nom} \end{bmatrix} \tag{24}$$

The state-space representation articulates the comprehensive system in the following way (25).

$$\begin{aligned} \dot{x} &= Ax + B_1 w + B_2 u \\ z_1 &+ C_1 x + D_{11} w + D_{12} u \\ z_2 &= C_2 x + C_{21} w + D_{22} u \end{aligned} \tag{25}$$

The state-space matrices are shown as (26).

$$\begin{bmatrix} A & B_1 & B_2 \\ C_1 & D_{11} & D_{12} \\ C_2 & C_{21} & C_{22} \end{bmatrix} = \begin{bmatrix} A_p & 0 & 0 & 0 & B_p \\ 0 & A_r & 0 & 0 & B_r \\ B_s C_p & 0 & A_s & 0 & 0 \\ 0 & C_r & 0 & 0 & D_r \\ 0 & 0 & C_s & 0 & 0 \\ C_p & 0 & 0 & I & 0 \end{bmatrix} \tag{26}$$

Using MATLAB's Robust Control Toolbox, the designed controller is computed based on these principles, resulting in the H_∞ controller defined by (27).

$$K(s) = \frac{17.78s^2 + 7.112s + 284.5}{s^2 + 3.2s + 16} \tag{27}$$

This controller was chosen during iterative testing to meet both performance and robustness criteria while ensuring little control effort. A parametric sweep was performed to assess robustness margins for varying fluid heights and container masses. The selected W_R was adjusted based on practical testing using system gain crossover analysis to balance reduction and strength across different model variables. Velocity transitions were implemented by the programming of three trajectory types in MATLAB/Simulink: step input, 5-second slope, and 2.5-second slope. These were implemented in the velocity reference transmitted to the motor model throughout the simulation loop. A second-order reference model processed the input profiles to simulate smooth motion behavior for comparison with the step disruption scenario.

V. Results of Simulation

This part talks about the simulation results of a sloshing dynamics system inside a cylinder-shaped container, looking at what happens when the input velocity changes and the liquid's height changes. Three input scenarios were assessed: a step input, a continuous function including 5-second gradients, and a modified acceleration profile with a 2.5-second gradient. The Integral of Absolute Error (IAE) and Root Mean Square Error (RMSE) were employed to assess performance. IAE and RMSE quantify the system's deviation from the input cumulatively and on average, respectively. Four unique liquid heights were simulated: 0.05 m, 0.10 m, 0.15 m, and 0.20 m. The results demonstrated that heightened liquid levels consistently led to more severe oscillations, extended settling times, and amplified error values. The consequences arise from heightened inertia and reduced damping at larger fluid masses, which impede the system's ability to accurately follow input trajectories. The results align with our expectations derived from the mechanical approximation approach employed to forecast natural frequency and sloshing amplitude patterns. They provide critical information for enhancing motion planning and system stability in fluid transport applications.

A. Analysis of Step Input Performance

The first experiment, illustrated in Fig. 9, investigates the sloshing dynamics under a velocity profile with a step input. The system's performance was measured using the IAE and RMSE metrics, which indicate cumulative and average errors, respectively. As shown in Table I, both measurements rise with increasing liquid height, indicating less system stability at elevated liquid levels.

The information shown in Fig. 9 and Table I shows that higher liquid levels (like 0.20 m) lead to stronger sloshing movements, which is indicated by increased displacement and angular amplitudes over time. This is also clear in the error measures, where both IAE and RMSE values increase along with the liquid height. This trend is also evident in the error measures, where both IAE and RMSE values rise proportionately with the liquid height. This observation aligns with the theoretical prediction that increased fluid mass results in greater inertia, thereby amplifying oscillatory tendencies.

The velocity profile for step input indicates that systems with reduced liquid levels exhibit faster recovery and less oscillatory deviations, hence enhancing tracking performance. These data suggest that under step input settings, smaller liquid heights provide enhanced control precision and less sloshing severity.

TABLE I. PERFORMANCE METRICS FOR SETPOINT 10 IN JOINT R

Metric	0.05	0.10	0.15	0.20
IAE (mm)	1.4621	3.4917	5.4966	7.4899
RMSE (mm)	0.0378	0.0926	0.1476	0.2026

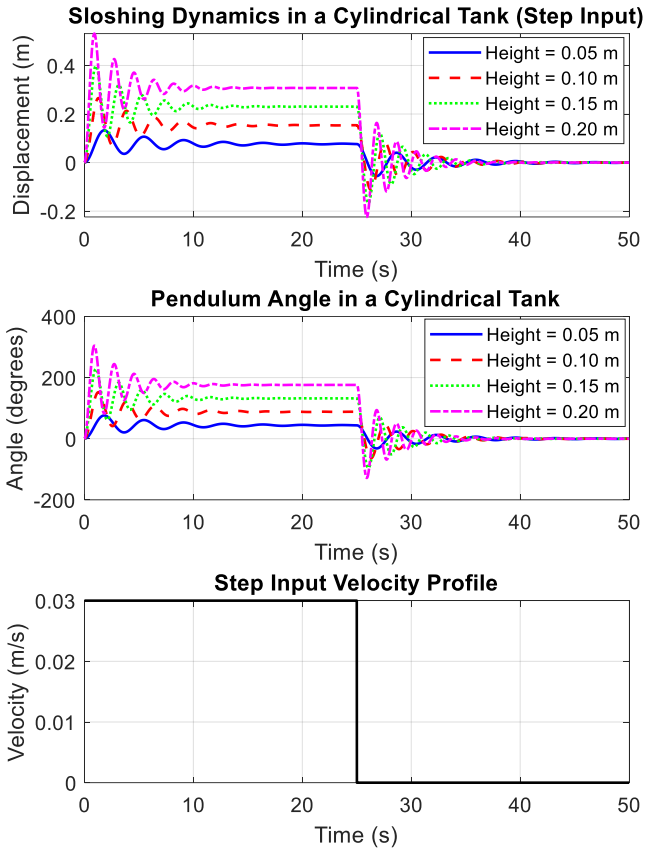

Fig. 9. Analysis of system response for setpoints

B. Analysis of Smooth Function Transitions

The second simulation, illustrated in Fig. 10, evaluates the system's performance using a smooth velocity profile characterized by acceleration and deceleration gradients of 5 seconds. The IAE and RMSE metrics were assessed at varying liquid heights, similar to the step input scenario. The results are presented in Table II.

The results shown in Fig. 10 and Table II show that both IAE and RMSE metrics go up a lot when the liquid level goes up, which means the system isn't working as well. The displacement and pendulum angle graphs further confirm that elevated liquid levels (e.g., 0.20 m) result in higher sloshing amplitude and prolonged settling times. In contrast, diminished liquid heights (e.g., 0.05 m) demonstrate improved stability and fewer oscillatory responses during movement. The continuous function input with a 5-second gradient is meant to lessen sudden changes, but bigger amounts of liquid cause more significant changes because they have more inertia. The discovery confirms theoretical predictions regarding the relationship between liquid inertia and control effectiveness.

TABLE II. PERFORMANCE METRICS FOR SMOOTH FUNCTION IN JOINT R

Metric	0.05	0.10	0.15	0.20
IAE (mm)	0.9874	2.4997	4.0505	5.5816
RMSE (mm)	0.0288	0.0752	0.1217	0.1682

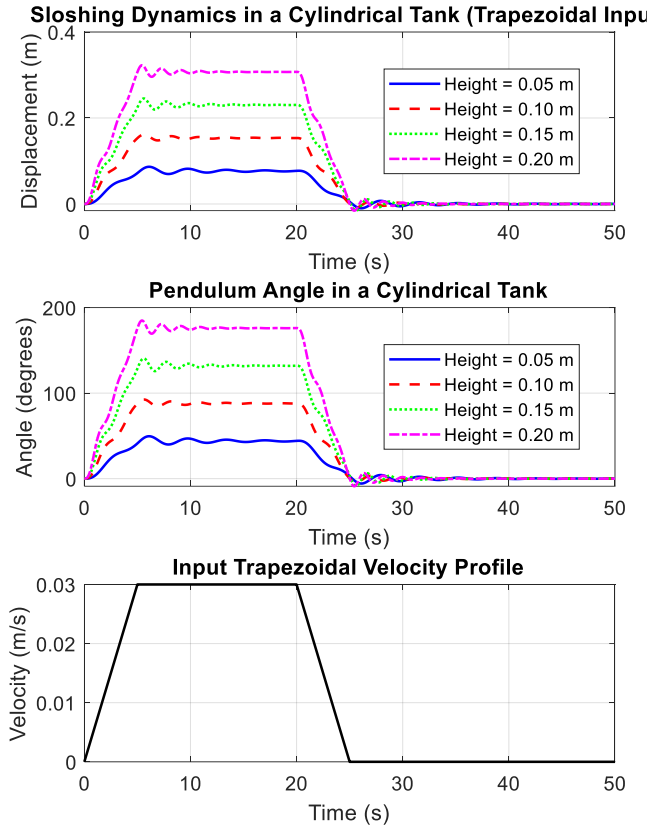

Fig. 10. Analysis of system response for smooth function and slop 2.5 s

C. Impact of Modified Acceleration Slope

The third simulation, seen in Fig. 11, analyzes the system's behavior when the acceleration and deceleration slopes of the velocity input are reduced to 2.5 seconds. The performance, evaluated at various liquid heights by IAE and RMSE metrics, is displayed in Table III.

Fig. 11 and Table III demonstrate that reducing the acceleration slope to 2.5 seconds does not lead to a decrease in IAE and RMSE metrics. In contrast, both error measures increase with rising liquid height, as indicated by the previous testing. The figures demonstrate that elevated liquid volumes (e.g., 0.20 m) result in heightened sloshing amplitudes and prolonged settling periods, despite the more uniform velocity profile. This result indicates that the effects of inertia are more important than how smooth the input profile is when there are large amounts of liquid. As the liquid level increases, the system's performance continues to decline. This evidence indicates that mass and sloshing dynamics significantly influence outcomes beyond merely altering the input.

TABLE III. PERFORMANCE METRICS FOR SMOOTH FUNCTION IN JOINT R

Metric	0.05	0.10	0.15	0.20
IAE (mm)	1.1634	2.8178	4.5747	6.3324
RMSE (mm)	0.0322	0.0821	0.1326	0.1832

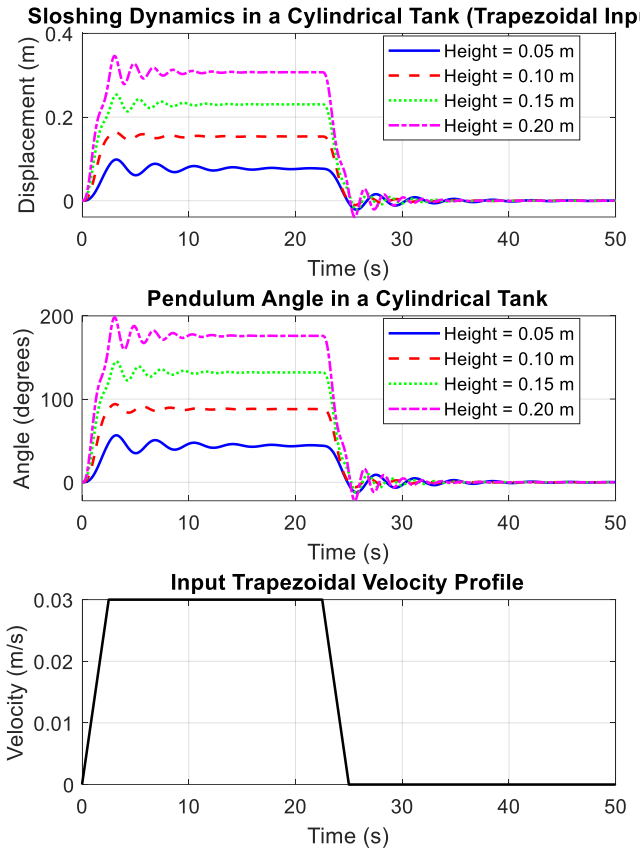

Fig. 11. Analysis of system response for smooth function and slop 2.5 s

D. Overall Summary

The simulation results unequivocally illustrate the influence of liquid height on sloshing dynamics and system stability within cylindrical containers. In all three investigations, the Integral of Absolute Error (IAE) and the Root Mean Square Error (RMSE) increased as the liquid height rose from 0.05 m to 0.20 m. These results consistently align with the expectations derived from the mechanical approximation model utilized in this study. The investigations encompassed a step input, a smooth velocity profile with 5-second slopes, and a modified acceleration slope of 2.5 seconds. This pattern indicates a deterioration in control function accompanied by increased fluid levels.

The step input example demonstrated that reduced liquid heights resulted in diminished oscillatory behavior and expedited stabilization, but increased liquid volumes led to more inertia, exacerbating sloshing and prolonging settling periods. The gradual alteration in the function accentuated this trend further; despite the gentler input, the additional mass at elevated liquid levels continued to diminish performance. In the third experiment, which had steeper slopes (2.5 s), it was shown that smoother input transitions did not alone make the unstable effects of higher liquid inertia less severe.

The statistics underscore that liquid height is a pivotal component affecting dynamic responsiveness. Decreased liquid heights lead to improved damping characteristics, lower sloshing amplitudes, and greater tracking accuracy across all velocity profiles. Thus, in the design of fluid handling systems, whether for robotics, automation, or medical transport, regulating liquid volume and system mass is essential for enhancing system resilience and performance in dynamic conditions.

VI. CONCLUSION

This research analyzed the sloshing dynamics in cylindrical containers influenced by varying liquid heights and input velocity patterns. The system's performance was evaluated using the Integral of Absolute Error (IAE) and Root Mean Square Error (RMSE). In all models, increased liquid levels consistently resulted in elevated sloshing amplitudes, prolonged settling durations, and enhanced tracking inaccuracies. The effects mostly arise from the heightened inertia of larger fluid masses, which limits the system's ability to rapidly adapt to dynamic fluctuations. Despite implementing moderate speed modifications to mitigate abrupt transitions, the findings indicated that these adjustments were insufficient to prevent oscillations under conditions of elevated fluid inertia. The research indicated that the liquid's height and density are crucial for maintaining system stability, with reduced liquid levels resulting in enhanced control, fewer oscillations, and improved accuracy in performance. These findings are particularly pertinent to fluid transport applications in robotics, logistics, and healthcare systems, where dynamic stability and accuracy are crucial. A notable drawback of this study is the lack of a comprehensive sensitivity analysis of the model parameters, namely the damping coefficient (B) and stiffness constant (K). These attributes substantially impact system dynamics and controller effectiveness. A thorough sensitivity analysis is recommended to investigate the impact of slight alterations in these parameters on sloshing dynamics, system responsiveness, and control robustness. This analysis would assist in delineating parameter boundaries and ensuring reliability amid real-world uncertainty. The modeling technique of this research is based on simplified assumptions, such as incompressible, inviscid, and irrotational flow conditions. While these assumptions facilitate a reasonable mathematical description, they may insufficiently capture the complexities of real fluid dynamics, including turbulence and viscosity. The H-infinity control strategy works well when uncertainties are known, but it can struggle in situations with strong nonlinearities or dynamic effects that haven't been considered. The findings of this study correspond with prior research, which indicated that sloshing behavior intensifies with increased liquid volume. This work integrates robust control techniques utilizing H-infinity methodologies, facilitating the management of disturbances across many scenarios. Future research should include testing in real-life situations, flexible and nonlinear control methods, and system designs tailored for different container shapes and fluid properties to improve these results. It is recommended to do sensitivity analysis and quantify uncertainty to optimize controller parameters and enhance system applicability in dynamic, real-world scenarios.

ACKNOWLEDGMENT

The researcher acknowledges the financial assistance the research team received from the research institute, academic services center, and college of biomedical engineering at Rangsit University. The Ethics Review Board of Rangsit University has evaluated the study, reference number RSUERB2025-006, and confirmed that the research does not involve human subjects. Moreover, AI-driven methods (QuillBot Premium) were utilized for grammatical verification, paraphrasing, and linguistic augmentation to ensure the accuracy and clarity of the text.

REFERENCES

[1] E. S. Ghith and F. A. A. Tolba, "Design and optimization of PID controller using various algorithms for micro-robotics system," *Journal of Robotics and Control (JRC)*, vol. 3, no. 3, pp. 244-256, 2022, doi: 10.18196/jrc.v3i3.14827.

[2] A. K. Hado, B. S. Bashar, M. M. A. Zahra, R. Alayi, Y. Ebazadeh, and I. Suwarno, "Investigating and optimizing the operation of microgrids with intelligent algorithms," *Journal of Robotics and Control (JRC)*, vol. 3, no. 3, pp. 279-288, 2022, doi: 10.18196/jrc.v3i3.14772.

[3] P. Chotikunnan *et al*., "Comparative Analysis of Sensor Fusion for Angle Estimation Using Kalman and Complementary Filters," *International Journal of Robotics and Control Systems*, vol. 5, no. 1, pp. 1–21, 2024, doi: 10.31763/ijrcs.v5i1.1674.

[4] A. Ma'arif and A. Çakan, "Simulation and arduino hardware implementation of dc motor control using sliding mode controller," *Journal of Robotics and Control (JRC)*, vol. 2, no. 6, pp. 582, 2021, doi: 10.18196/jrc.26140.

[5] A. Ma'arif and N. R. Setiawan, "Control of DC motor using integral state feedback and comparison with PID: simulation and Arduino implementation," *Journal of Robotics and Control (JRC)*, vol. 2, no. 5, pp. 456-461, 2021, doi: 10.18196/jrc.25122.

[6] H. Maghfiroh, A. Ramelan, and F. Adriyanto, "Fuzzy-PID in BLDC motor speed control using MATLAB/Simulink," *Journal of Robotics and Control (JRC)*, vol. 3, no. 1, pp. 8-13, 2022, doi: 10.18196/jrc.v3i1.10964.

[7] M. Samuel, M. Mohamad, M. Hussein, and S. M. Saad, "Lane keeping maneuvers using proportional integral derivative (PID) and model predictive control (MPC)," *Journal of Robotics and Control (JRC)*, vol. 2, no. 2, pp. 78-82, 2021, doi: 10.18196/jrc.2256.

[8] A. Wajiansyah, S. Supriadi, A. F. O. Gaffar, and A. B. W. Putra, "Modeling of 2-DOF hexapod leg using analytical method," *Journal of Robotics and Control (JRC)*, vol. 2, no. 5, pp. 435-440, 2021, doi: 10.18196/jrc.25119.

[9] R. P. Borase, D. K. Maghade, S. Y. Sondkar, and S. N. Pawar, "A review of PID control, tuning methods and applications," *International Journal of Dynamics and Control*, vol. 9, pp. 818-827, 2021, doi: 10.1007/s40435-020-00665-4.

[10] Z. Dachang, D. Baolin, Z. Puchen, and C. Shouyan, "Constant force PID control for robotic manipulator based on fuzzy neural network algorithm," *Complexity*, vol. 2020, 2020, doi: 10.1155/2020/3491845.

[11] B. Li, Y. Tan, J. Chen, X. Liu, and S. Yang, "Precise active seeding downforce control system based on fuzzy PID," *Mathematical Problems in Engineering*, vol. 2020, 2020, doi: 10.1155/2020/5123830.

[12] E. S. Rahayu, A. Ma'arif, and A. Çakan, "Particle Swarm Optimization (PSO) Tuning of PID Control on DC Motor," *International Journal of Robotics and Control Systems*, vol. 2, no. 2, pp. 435–447, 2022, doi: 10.31763/ijrcs.v2i2.476.

[13] Z. Qi, Q. Shi, and H. Zhang, "Tuning of Digital PID Controllers Using Particle Swarm Optimization Algorithm for a CAN-Based DC Motor Subject to Stochastic Delays," *IEEE Transactions on Industrial Electronics*, vol. 67, no. 7, pp. 5637–5646, 2020, doi: 10.1109/TIE.2019.2934030.

[14] S. Mahfoud, A. Derouich, N. El Ouanjli, M. El Mahfoud, and M. Taoussi, "A New Strategy-Based PID Controller Optimized by Genetic Algorithm for DTC of the Doubly Fed Induction Motor," *Systems*, vol. 9, no. 2, p. 37, 2021, doi: 10.3390/systems9020037.

[15] M. M. Nishat *et al*., "Development of Genetic Algorithm (GA) Based Optimized PID Controller for Stability Analysis of DC-DC Buck Converter," *Journal of Power and Energy Engineering*, vol. 8, no. 09, p. 8, 2020, doi: 10.4236/jpee.2020.89002.

[16] R. Kristiyono and W. Wiyono, "Autotuning Fuzzy PID Controller for Speed Control of BLDC Motor," *Journal of Robotics and Control*, vol. 2, no. 5, pp. 400–407, 2021, doi: 10.18196/jrc.25114.

[17] G. B. So, "A modified 2-DOF control framework and GA based intelligent tuning of PID controllers," *Processes*, vol. 9, no. 3, p. 423, 2021, doi: 10.3390/pr9030423.

[18] P. K. Dash, S. Mishra, M. A. Salama, and A. C. Liew, "Classification of power system disturbances using a fuzzy expert system and a Fourier linear combiner," *IEEE Transactions on Power Delivery*, vol. 15, no. 2, pp. 472-477, Apr. 2000, doi: 10.1109/61.852971.

[19] K. Kunhimangalam, S. Ovallath, and P. K. Joseph, "A novel fuzzy expert system for the identification of severity of carpal tunnel syndrome," *BioMed research international*, vol. 2013, pp. 1-12, 2013, doi: 10.1155/2013/846780.

[20] L. Ali *et al*., "An optimized stacked support vector machines based expert system for the effective prediction of heart failure," *IEEE Access*, vol. 7, pp. 54007-54014, 2019, doi: 10.1109/ACCESS.2019.2909969.

[21] R. H. Faisal *et al*., "A modular fuzzy expert system for chemotherapy drug dose scheduling," *Healthcare Analytics*, vol. 3, p. 100139, 2023, doi: 10.1016/j.health.2023.100139.

[22] E. Pawan, R. M. Thamrin, W. Widodo, S. H. B. S. H. Bei, and J. J. Luanmasa, "Implementation of Forward Chaining Method in Expert System to Detect Diseases in Corn Plants in Muara Tami District," *International Journal of Computer and Information System (IJCIS)*, vol. 3, no. 1, pp. 27-33, 2022, doi: 10.29040/ijcis.v3i1.59.

[23] H. Li *et al*., "Supportive emergency decision-making model towards sustainable development with fuzzy expert system," *Neural Computing & Applications*, vol. 33, pp. 15619–15637, 2021, doi: 10.1007/s00521-021-06183-4.

[24] H. Pievtsov *et al*., "Development of an advanced method of finding solutions for neuro-fuzzy expert systems of analysis of the radio electronic situation," *EUREKA: Physics and Engineering*, no. 4, pp. 78–89, 2020, doi: 10.21303/2461-4262.2020.001353.

[25] E. A. Algehyne, M. L. Jibril, N. A. Algehainy, O. A. Alamri, and A. K. Alzahrani, "Fuzzy neural network expert system with an improved Gini index random forest-based feature importance measure algorithm for early diagnosis of breast cancer in Saudi Arabia," *Big Data and Cognitive Computing*, vol. 6, no. 1, pp. 13, Jan. 2022, doi: 10.3390/bdcc6010013.

[26] L. J. Muhammad and E. A. Algehyne, "Fuzzy-based expert system for diagnosis of coronary artery disease in Nigeria," *Health Technology*, vol. 11, pp. 319–329, 2021, doi: 10.1007/s12553-021-00531-z.

[27] J. Singla *et al*., "Research Article A Novel Fuzzy Logic-Based Medical Expert System for Diagnosis of Chronic Kidney Disease," *Mobile Information Systems*, vol. 2020, 2020, doi: 10.1155/2020/8887627.

[28] P. Chotikunnan and Y. Pititheeraphab, "Adaptive P Control and Adaptive Fuzzy Logic Controller with Expert System Implementation for Robotic Manipulator Application," *Journal of Robotics and Control (JRC)*, vol. 4, no. 2, pp. 217-226, 2023, doi: 10.18196/jrc.v4i2.17757

[29] P. Chotikunnan, T. Puttasakul, R. Chotikunnan, B. Panomruttanarug, M. Sangworasil, and A. Srisiriwat, "Evaluation of Single and Dual image Object Detection through Image Segmentation Using ResNet18 in Robotic Vision Applications," *Journal of Robotics and Control (JRC)*, vol. 4, no. 3, pp. 263–277, Apr. 2023, doi: 10.18196/jrc.v4i3.17932

[30] M. Raihan *et al*., "Development of a smartphone-based expert system for COVID-19 risk prediction at early stage," *IEEE Journal of Biomedical and Health Informatics*, vol. 26, no. 11, pp. 3448-3459, Nov. 2022, doi: 10.3390/bioengineering9070281

[31] S. A. Abdymanapov, M. Muratbekov, S. Altynbek, and A. Barlybayev, "Fuzzy expert system of information security risk assessment on the example of analysis learning management systems," *IEEE Access*, vol. 9, pp. 156556–156565, 2021, doi: 10.1109/ACCESS.2021.3129488.

[32] A. Shuraiji and S. Shneen, "Fuzzy Logic Control and PID Controller for Brushless Permanent Magnetic Direct Current Motor: A Comparative Study," *Journal of Robotics and Control (JRC)*, vol. 3, no. 6, pp. 762–768, 2022, doi: 10.18196/jrc.v3i6.15974

[33] K. Lee, D. Y. Im, B. Kwak, and Y. J. Ryoo, "Design of fuzzy-PID controller for path tracking of mobile robot with differential drive," *International Journal of Fuzzy Logic and Intelligent Systems*, vol. 18, no. 3, pp. 220–228, 2018, doi: 10.5391/IJFIS.2018.18.3.220

[34] M. A. Abdelghany, A. O. Elnady, and S. O. Ibrahim, "Optimum PID Controller with Fuzzy Self-Tuning for DC Servo Motor," *Journal of Robotics and Control (JRC)*, vol. 4, no. 4, pp. 500-508, 2023, doi: 10.18196/jrc.v4i4.18676

[35] Z. Wang, L. Zou, X. Su, G. Luo, R. Li, and Y. Huang, "Hybrid force/position control in workspace of robotic manipulator in uncertain environments based on adaptive fuzzy control," *Robotics and Autonomous Systems*, vol. 145, p. 103870, 2021, doi: 10.1016/j.robot.2021.103870.

[36] T. A. Lin, Y. C. Lee, W. J. Chang, and Y. H. Lin, "Robust Observer-Based Proportional Derivative Fuzzy Control Approach for Discrete-Time Nonlinear Descriptor Systems with Transient Response Requirements," *Processes*, vol. 12, no. 3, p. 540, 2024, doi: 10.3390/pr12030540.

[37] D. A. Pham and S. H. Han, "Enhancing Underwater Robot Manipulators with a Hybrid Sliding Mode Controller and Neural-Fuzzy Algorithm," *Journal of Marine Science and Engineering*, vol. 11, no. 12, p. 2312, 2023, doi: 10.3390/jmse11122312.

[38] J. Han, F. Wang, and C. Sun, "Trajectory Tracking Control of a Manipulator Based on an Adaptive Neuro-Fuzzy Inference System," *Applied Sciences*, vol. 13, no. 2, p. 1046, 2023, doi: 10.3390/app13021046.

[39] M. Singh, S. Arora, and O. Shah, "Enhancing Hybrid Power System Performance with GWO-Tuned Fuzzy-PID Controllers: A Comparative Study," *International Journal of Robotics and Control Systems*, vol. 4, no. 2, pp. 709–726, 2024, doi: 10.31763/ijrcs.v4i2.1388.

[40] M. Mukhtar, D. Khudher, and T. Kalganova, "A control structure for ambidextrous robot arm based on Multiple Adaptive Neuro-Fuzzy Inference System," *IET Control Theory and Applications*, vol. 15, no. 11, pp. 1518–1532, 2021, doi: 10.1049/cth2.12140.

[41] B. Saeedi, M. M. Moghaddam, and M. Sadedel, "Inverse kinematics analysis of a wrist rehabilitation robot using artificial neural network and adaptive Neuro-Fuzzy inference system," *Mechanics Based Design of Structures and Machines*, pp. 1–49, 2024, doi: 10.1080/15397734.2024.2356066.

[42] O. Elhaki *et al*., "Robust amplitude-limited interval type-3 neuro-fuzzy controller for robot manipulators with prescribed performance by output feedback," *Neural Computing and Applications*, vol. 35, pp. 9115–9130, 2023, doi: 10.1007/s00521-022-08174-5.

[43] H. Batti, C. Ben Jabeur, and H. Seddik, "Autonomous smart robot for path predicting and finding in maze based on fuzzy and neuro-fuzzy approaches," *Asian Journal of Control*, vol. 23, no. 1, pp. 3–12, 2021, doi: 10.1002/asjc.2345.

[44] Y. Chen, B. Chu, and C. T. Freeman, "Iterative learning control for robotic path following with trial-varying motion profiles," *IEEE/ASME Transactions on Mechatronics*, vol. 27, no. 6, pp. 4697–4706, 2022, doi: 10.1109/TMECH.2022.3164101.

[45] Y. Wu, M. Yang, and J. Zhang, "Open-Closed-Loop Iterative Learning Control with the System Correction Term for the Human Soft Tissue Welding Robot in Medicine," *Mathematical Problems in Engineering*, vol. 2020, p. 2458318, 2020, doi: 10.1155/2020/2458318.

[46] X. Yu, Z. Hou, M. M. Polycarpou, and L. Duan, "Data-driven iterative learning control for nonlinear discrete-time MIMO systems," *IEEE Transactions on Neural Networks and Learning Systems*, vol. 32, no. 3, pp. 1136–1148, 2020, doi: 10.1109/TNNLS.2020.2980588.

[47] H.-T. Nguyen *et al*., "Experiment Ball Levitation with Fuzzy PID and PID Implementation," *Journal of Fuzzy Systems and Control*, vol. 2, no. 3, pp. 129–134, 2024, doi: 10.59247/jfsc.v2i3.221.

[48] F. Z. Baghli, Y. Lakhal, and Y. A. El Kadi, "The Efficiency of an Optimized PID Controller Based on Ant Colony Algorithm (ACO-PID) for the Position Control of a Multi-articulated System," *Journal of Robotics and Control (JRC)*, vol. 4, no. 3, pp. 289-298, 2023, doi: 10.18196/jrc.v4i3.17709.

[49] S. N. Silva, F. F. Lopes, C. Valderrama, and M. A. Fernandes, "Proposal of Takagi–Sugeno fuzzy-PI controller hardware," *Sensors*, vol. 20, no. 7, p. 1996, 2020, doi: 10.3390/s20071996.

[50] S. Ayub, N. Singh, M. Z. Hussain, M. Ashraf, D. K. Singh, and A. Haldorai, "Hybrid approach to implement multi-robotic navigation system using neural network, fuzzy logic, and bio-inspired optimization methodologies," *Computational Intelligence*, vol. 39, no. 4, pp. 592–606, 2023, doi: 10.1111/coin.12547.

[51] O. Lamine *et al*., "A Combination of INC and Fuzzy Logic-Based Variable Step Size for Enhancing MPPT of PV Systems," *International Journal of Robotics and Control Systems*, vol. 4, no. 2, pp. 877–892, 2024, doi: 10.31763/ijrcs.v4i2.1428.

[52] N. Jamali, M. Gharib, and B. Omidi Koma, "Neuro-Fuzzy Decision Support System for Optimization of the Indoor Air Quality in Operation Rooms," *International Journal of Robotics and Control Systems*, vol. 3, no. 1, pp. 98–106, 2023, doi: 10.31763/ijrcs.v3i1.854.

[53] S. Nemmour, B. Daaou, and F. Okello, "Fuzzy Control for Spacecraft Orbit Transfer with Gain Perturbations and Input Constraint," *International Journal of Robotics and Control Systems*, vol. 4, no. 4, pp. 1561–1583, 2024, doi: 10.31763/ijrcs.v4i4.1549.

[54] C. Deniz and G. Gökmen, "A new robotic application for covid-19 specimen collection process," *Journal of Robotics and Control (JRC)*, vol. 3, no. 1, pp. 73-77, 2022, doi: 10.18196/jrc.v3i1.11659.

[55] A. R. Al Tahtawi, M. Agni, and T. D. Hendrawati, "Small-scale robot arm design with pick and place mission based on inverse kinematics," *Journal of Robotics and Control (JRC)*, vol. 2, no. 6, pp. 469-475, 2021, doi: 10.18196/jrc.26124.

[56] M. Marsono, Y. Yoto, A. Suyetno, and R. Nurmalasari, "Design and programming of 5 axis manipulator robot with GrblGru open source software on preparing vocational students' robotic skills," *Journal of Robotics and Control (JRC)*, vol. 2, no. 6, pp. 539-545, 2021, doi: 10.18196/jrc.26134.

[57] K. Lee, C. Jung, and W. Chung, "Accurate calibration of kinematic parameters for two wheel differential mobile robots," *Journal of Mechanical Science and Technology*, vol. 25, pp. 1603–1611, 2011, doi: 10.1007/s12206-011-0334-y.

[58] P. Minyong, *Motion control of mechatronics systems concerning with multi-fingered robot hand and transfer system of linear motor*, Ph.D. dissertation, Toyohashi University of Technology, Japan, 2004.

[59] J. Kern, D. Marrero, and C. Urrea, "Fuzzy control strategies development for a 3-DoF robotic manipulator in trajectory tracking," *Processes*, vol. 11, no. 12, p. 3267, 2023, doi: 10.3390/pr11123267.

[60] M. H. Barhaghtalab, M. A. Sepestanaki, S. Mobayen, A. Jalilvand, A. Fekih, and V. Meigoli, "Design of an adaptive fuzzy-neural inference system-based control approach for robotic manipulators," *Applied Soft Computing*, vol. 149, p. 110970, 2023, doi: 10.1016/j.asoc.2023.110970.

[61] P. Chotikunnan *et al*., "Genetic Algorithm-Optimized LQR for Enhanced Stability in Self-Balancing Wheelchair Systems," *Control Systems and Optimization Letters*, vol. 2, no. 3, pp. 327–335, 2024, doi: 10.59247/csol.v2i3.161.

[62] D. T. Tran, N. M. Hoang, N. H. Loc, Q. T. Truong, and N. T. Nha, "A Fuzzy LQR PID Control for a Two-Legged Wheel Robot with Uncertainties and Variant Height," *Journal of Robotics and Control (JRC)*, vol. 4, no. 5, pp. 612-620, 2023, doi: 10.18196/jrc.v4i5.19448

[63] P. Chotikunnan and R. Chotikunnan, "Dual Design PID Controller for Robotic Manipulator Application," *Journal of Robotics and Control (JRC)*, vol. 4, no. 1, pp. 23–34, Feb. 2023, doi: 10.18196/jrc.v4i1.16990.

[64] P. Chotikunnan, R. Chotikunnan, and P. Minyong, "Adaptive Parallel Iterative Learning Control with A Time-Varying Sign Gain Approach Empowered by Expert System," *Journal of Robotics and Control (JRC)*, vol. 5, no. 1, pp. 72–81, Jan. 2024, doi: 10.18196/jrc.v5i1.20890.

[65] P. Chotikunnan, R. Chotikunnan, A. Nirapai, A. Wongkamhang, P. Imura, and M. Sangworasil, "Optimizing Membership Function Tuning for Fuzzy Control of Robotic Manipulators Using PID-Driven Data Techniques," *Journal of Robotics and Control (JRC)*, vol. 4, no. 2, pp. 128–140, Mar. 2023, doi: 10.18196/jrc.v4i2.18108.

[66] K. Li and Y. Li, "Fuzzy adaptive optimal consensus fault-tolerant control for stochastic nonlinear multiagent systems," *IEEE Transactions on Fuzzy Systems*, vol. 30, no. 8, pp. 2870–2885, 2021, doi: 10.1109/TFUZZ.2021.3094716.

[67] X. Tang, D. Ning, H. Du, W. Li, Y. Gao, and W. Wen, "A Takagi-Sugeno fuzzy model-based control strategy for variable stiffness and variable damping suspension," *IEEE Access*, vol. 8, pp. 71628–71641, 2020, doi: 10.1109/ACCESS.2020.2983998.

[68] M. S. Gharajeh and H. B. Jond, "Hybrid global positioning system-adaptive neuro-fuzzy inference system based autonomous mobile robot navigation," *Robotics and Autonomous Systems*, vol. 134, p. 103669, 2020, doi: 10.1016/j.robot.2020.103669.

[69] C. Kahraman, M. Deveci, E. Boltürk, and S. Türk, "Fuzzy controlled humanoid robots: A literature review," *Robotics and Autonomous Systems*, vol. 134, p. 103643, 2020, doi: 10.1016/j.robot.2020.103643.

[70] N. Y. Allagui, F. A. Salem, and A. M. Aljuaid, "Artificial Fuzzy-PID Gain Scheduling Algorithm Design for Motion Control in Differential Drive Mobile Robotic Platforms," *Computational Intelligence and*

Neuroscience, vol. 2021, no. 1, p. 5542888, 2021, doi: 10.1155/2021/5542888.

[71] E. Xidias, V. Moulianitis, and P. Azariadis, "Optimal robot task scheduling based on adaptive neuro-fuzzy system and genetic algorithms," *The International Journal of Advanced Manufacturing Technology*, vol. 115, pp. 927–939, 2021, doi: 10.1007/s00170-020-06166-0.

[72] M. H. Haider *et al*., "Robust mobile robot navigation in cluttered environments based on hybrid adaptive neuro-fuzzy inference and sensor fusion," *Journal of King Saud University - Computer and Information Sciences*, vol. 34, no. 10, pp. 9060–9070, 2022, doi: 10.1016/j.jksuci.2022.08.031.

[73] C. Dumitrescu, P. Ciotirnae, and C. Vizitiu, "Fuzzy logic for intelligent control system using soft computing applications," *Sensors*, vol. 21, no. 8, p. 2617, 2021, doi: 10.3390/s21082617.

[74] I. Zaitceva and B. Andrievsky, "Methods of intelligent control in mechatronics and robotic engineering: A survey," *Electronics*, vol. 11, no. 15, p. 2443, 2022, doi: 10.3390/electronics11152443.

[75] R. Chotikunnan, P. Chotikunnan, A. Ma'arif, N. Thongpance, Y. Pititheeraphab, and A. Srisiriwat, "Ball and Beam Control: Evaluating Type-1 and Interval Type-2 Fuzzy Techniques with Root Locus Optimization," *International Journal of Robotics and Control Systems*, vol. 3, no. 2, pp. 286–303, 2023, doi: 10.31763/ijrcs.v3i2.997.

[76] T. Ngo, T. Tran, T. Le, and B. Lam, "An Application of Modified T2FHC Algorithm in Two-Link Robot Controller," *Journal of Robotics and Control*, vol. 4, no. 4, pp. 509–520, 2023, doi: 10.18196/jrc.v4i4.18943.

[77] R. Chotikunnan, P. Chotikunnan, Y. Pititheeraphab, and P. Minyong, "Time-Varying Sign Gain with Expert System in Serial Iterative Learning Control Architecture," *International Review of Automatic Control (IREACO)*, vol. 17, no. 1, p. 1, Jan. 2024, doi: 10.15866/ireaco.v17i1.24739.

[78] P. Chotikunnan and B. Panomruttanarug, "Time-varying learning control design using fuzzy logic control for robotic manipulators: Serial and parallel ILC configurations," *Journal of Intelligent & Fuzzy Systems*, vol. 43, no. 3, pp. 2419–2434, 2022, doi: 10.3233/JIFS-213082.

[79] H. Chaudhary, V. Panwar, N. Sukavanam, and B. Chahar, "Imperialist Competitive Algorithm Optimised Adaptive Neuro Fuzzy Controller for Hybrid Force Position Control of an Industrial Robot Manipulator: A Comparative Study," *Fuzzy Information and Engineering*, vol. 12, no. 4, pp. 435–451, Dec. 2020, doi: 10.1080/16168658.2021.1921378.

[80] S. Primatesta, L. O. Russo, and B. Bona, "Dynamic trajectory planning for mobile robot navigation in crowded environments," *in Proceedings of the 2016 IEEE 21st International Conference on Emerging Technologies and Factory Automation (ETFA)*, Berlin, Germany, Sep. 2016, pp. 1–8, doi: 10.1109/ETFA.2016.7733510.

[81] H. Abdelfattah, S. Kotb, M. Esmail, and M. Mosaad, "Adaptive Neuro-Fuzzy Self Tuned-PID Controller for Stabilization of Core Power in a Pressurized Water Reactor," *International Journal of Robotics and Control Systems*, vol. 3, no. 1, pp. 1–18, 2022, doi: 10.31763/ijrcs.v3i1.710.

[82] Z. A. Al-Dabbagh, S. W. Shneen, and A. O. Hanfesh, "Fuzzy Logic-based PI Controller with PWM for Buck-Boost Converter," *Journal of Fuzzy Systems and Control*, vol. 2, no. 3, pp. 147–159, 2024, doi: 10.59247/jfsc.v2i3.239.

[83] S. Palanisamy and J. Periyasamy, "Interval-Valued Intuitionistic Fuzzy Cosine Similarity Measures for Real World Problem Solving," *International Journal of Robotics and Control Systems*, vol. 4, no. 2, pp. 655–677, 2024, doi: 10.31763/ijrcs.v4i2.1251.

[84] K. A. Al Sumarmad, N. Sulaiman, N. I. A. Wahab, and H. Hizam, "Energy management and voltage control in microgrids using artificial neural networks, PID, and fuzzy logic controllers," *Energies*, vol. 15, no. 1, p. 303, 2022, doi: 10.3390/en15010303.

[85] Y. Chuang, M. Herrera, and A. Balal, "Using PV Fuzzy Tracking Algorithm to Charge Electric Vehicles," *International Journal of Robotics and Control Systems*, vol. 2, no. 2, pp. 253–261, 2022, doi: 10.31763/ijrcs.v2i2.636.

[86] D. Yu, C. P. Chen, and H. Xu, "Fuzzy swarm control based on sliding-mode strategy with self-organized omnidirectional mobile robots system," *IEEE Transactions on Systems, Man, and Cybernetics: Systems*, vol. 52, no. 4, pp. 2262–2274, 2021, doi: 10.1109/ACCESS.2020.2984695.